Title

The p80 homology region of TEP1 is sufficient for its association with the telomerase and vault RNAs, and the vault particle.

Journal

Nucleic acids research, 33(3)

ISSN

0305-1048

Authors

Poderycki, Michael J
Rome, Leonard H
Harrington, Lea
et al.

Publication Date

2005

DOI

10.1093/nar/gki234

Peer reviewed

Nucleic Acids Research, 2005, Vol. 33, No. 3 ***893–902***
doi:10.1093/nar/gki234

The p80 homology region of TEP1 is sufficient for its association with the telomerase and vault RNAs, and the vault particle

Michael J. Poderycki, Leonard H. Rome, Lea Harrington[1] and Valerie A. Kickhoefer*

Department of Biological Chemistry and the Jonsson Comprehensive Cancer Center, The David Geffen School of Medicine at UCLA, 10833 Le Conte Avenue, Los Angeles, CA 90095-1737, USA and [1]Department of Medical Biophysics, Ontario Cancer Institute, University of Toronto, 620 University Avenue, Toronto, Ontario M5G 2C1, Canada

Received November 12, 2004; Revised January 10, 2005; Accepted January 20, 2005

ABSTRACT

TEP1 is a protein component of two ribonucleoprotein complexes: vaults and telomerase. The vault-associated small RNA, termed vault RNA (VR), is dependent upon TEP1 for its stable association with vaults, while the association of telomerase RNA with the telomerase complex is independent of TEP1. Both of these small RNAs have been shown to interact with amino acids 1–871 of TEP1 in an indirect yeast three-hybrid assay. To understand the determinants of TEP1–RNA binding, we generated a series of TEP1 deletions and show by yeast three-hybrid assay that the entire *Tetrahymena* p80 homology region of TEP1 is required for its interaction with both telomerase and VRs. This region is also sufficient to target the protein to the vault particle. Electrophoretic mobility shift assays using the recombinant TEP1 RNA-binding domain (TEP1–RBD) demonstrate that it binds RNA directly, and that telomerase and VRs compete for binding. VR binds weakly to TEP1–RBD *in vitro*, but mutation of VR sequences predicted to disrupt helices near its central loop enhances binding. Antisense oligonucleotide-directed RNase H digestion of endogenous VR indicates that this region is largely single stranded, suggesting that TEP1 may require access to the VR central loop for efficient binding.

INTRODUCTION

Vaults are 13 million Dalton ribonucleoprotein particles (RNPs) of unknown function with dimensions of 42 × 75 nm (1–3). Vault morphology is reminiscent of a barrel with a cap on each end and is highly conserved across a wide range of species. The basic vault structure is formed by multimerization of a predicted 96 copies of the 96 kDa major vault protein (MVP), which makes up >70% of the particle mass and forms the entire exterior shell of vaults (4). Virtually all of the MVPs of the cell biochemically fractionate as a large particle, suggesting that all or most MVP monomers are incorporated into vaults. Although the function of vaults has not been determined, roles have been proposed with respect to nucleocytoplasmic trafficking, multi-drug resistance and, more recently, as a scaffold for epidermal growth factor signaling (5–9). Despite their presence in a wide variety of evolutionarily diverse organisms and upregulation in several multi-drug resistant cancer cell lines, mammalian vaults are not required for survival, as mice lacking MVP are viable, do not display increased sensitivity to cytostatic drugs, and have no obvious phenotypic defects (10).

Vaults contain two other proteins: vault poly (ADP-ribose) polymerase (VPARP) and telomerase-associated protein 1 (TEP1), as well as a small untranslated vault RNA (VR) (11–13). Each of these components is present in multiple copies in vaults, but their precise stoichiometry with respect to a single vault is unclear, and it is not known whether all vaults contain equal numbers of these components. Moreover, some species, such as human and bullfrog, express multiple-related VRs that can associate with the vault particle (8,11). Cryoelectron microscope (cryoEM) image reconstructions of intact or RNase-treated vaults purified from rat liver have resolved the structure to 31 and 22 Å resolutions, respectively. Difference imaging between intact and RNase-treated vaults localizes VR to the interior ends of each of the vault caps (3,14). The precise localization of VPARP and TEP1 within the vault particle is not yet known. Both proteins, as well as VR, are also found in non-vault-associated fractions within the cell (8,12,13).

*To whom correspondence should be addressed. Tel: +1 310 794 4873; Fax: +1 310 206 5272; Email: vkick@mednet.ucla.edu

TEP1 is an RNA-binding protein that interacts with mammalian telomerase in cell extracts and was cloned based upon its homology with *Tetrahymena* p80, which also co-purified with telomerase activity and binds the *Tetrahymena* telomerase RNA (TR) *in vitro* (15–17). A schematic illustration of the various domains identified in TEP1 is shown in Figure 1. Disruption of the p80/p95 complex in *Tetrahymena* leads to telomere lengthening (18). However, p80 is not a core telomerase component and is not required for telomerase activity (18–20). Furthermore, recombinant p80 binds poorly or not at all to other co-expressed telomerase subunits in *Escherichia coli* or insect cell extracts and non-specifically interacts with a number of RNAs *in vitro*, in addition to its interaction with TR (19). The precise function of mammalian TEP1 is also not known, but it has been shown to be one of four components of purified vaults and to interact with the VR and mammalian TR in an indirect yeast three-hybrid assay (13,16). Immunoprecipitation of endogenous TEP1 co-immunoprecipitates telomerase activity (16,17). Despite the *in vitro* association between TEP1 and telomerase activity, Tep1-deficient mice have no known telomerase-related defect, as telomerase activity, TR levels and telomere length are normal in these mice (21,22). However, VR levels are reduced in all tissues studied from Tep1-deficient mice and VR stability is markedly reduced in mouse embryonic fibroblasts (MEFs) derived from these mice in comparison with MEFs derived from wild-type mice. Furthermore, vaults purified from Tep1-deficient mice do not contain VR, demonstrating genetically and biochemically that TEP1 is required for the association of VR with the vault particle (22).

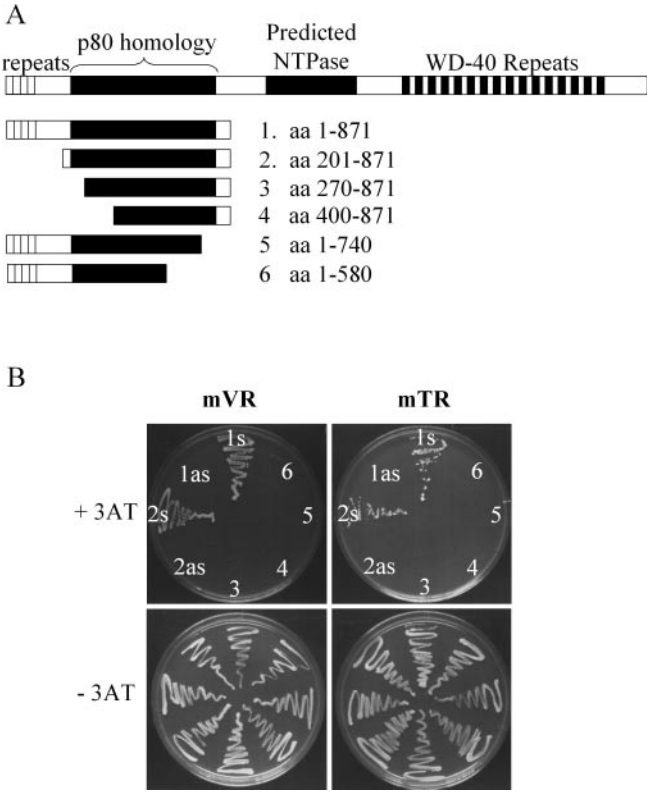

Figure 1. Yeast three-hybrid analysis of TEP1 deletions and vault/telomerase RNAs. (**A**) TEP1 truncations were made using amino acids 1–871 as a starting point, since this region of human TEP1 interacts with human vault and telomerase RNAs in the yeast three-hybrid system (16). (**B**) Yeast strain L40i was transformed with plasmids expressing the above TEP1 deletions and murine vault or telomerase RNA in either sense (s) or antisense (as) orientations. Yeast were grown on synthetic drop-out plates lacking uracil, leucine and histidine, and containing 5 mM 3-aminotriazole (+3AT) or synthetic media lacking only uracil and leucine (−3AT). Growth on +3AT media indicates a TEP1–RNA interaction. No TEP1 deletions interacted with antisense RNA constructs (data not shown), but this is shown above only for those TEP1 deletions that interact with RNA in the sense orientation (constructs 1 and 2).

VPARP is a member of the PARP family of proteins and is the only vault-associated protein demonstrated to have enzymatic activity, as it is able to ADP-ribosylate both itself and MVP *in vitro*, although the functional significance of this modification is not known (12). In addition to its localization in the vault particle, VPARP is seen at the mitotic spindle using immunofluorescence, and immunoprecipitation of VPARP from lysates derived from VPARP transfected cells results in the co-immunoprecipitation of telomerase activity (12,23). Like TEP1, Vparp-deficient mice also have no known phenotypic defects, telomerase-related or otherwise (22,23). Vaults purified from livers of either Vparp- or Tep1-deficient mice also appear morphologically normal (22,23).

VR is an RNA polymerase III transcript that does not appear to be further processed, and thus retains its 3′ polyuridylate tail, binds the La autoantigen *in vitro* and is found stably complexed with La apart from the vault particle *in vivo* (24). Interestingly, La has also been found to co-purify with vaults purified from rat livers. The genes for VR have been identified and sequenced for a variety of species, and the RNAs are all predicted to fold into a highly conserved structure (8,25). Some species, such as humans and bullfrogs, express multiple-related VRs, and two species, humans and mouse, each contains a VR pseudogene (8,25,26). The function of VR is not known, but as it is unimportant for the structural integrity of the vault particle, it is proposed to play a functional rather than structural role in the complex (14,27).

The goal of the current study is to determine whether TEP1, a component of both vault and telomerase RNPs, each containing an unrelated RNA, VR or TR, binds singly or simultaneously to these RNA species. Using the yeast three-hybrid system, we determined that the entire TEP1 *Tetrahymena* p80 homology region is required for its interaction with VR and TR. Electrophoretic mobility shift assays (EMSAs) using a partially purified truncation of TEP1 containing this RNA-binding domain (TEP1–RBD) demonstrate that TEP1 can indeed bind RNA directly, and that, like p80, TEP1 also binds some RNAs non-specifically. However, although TR binds to TEP1–RBD *in vitro*, only point mutants of mVR that are predicted to disrupt base-pairing near the VR central loop were able to interact with TEP1–RBD, suggesting that other factors are normally required for this association. Furthermore, competition experiments indicate that there is likely only one RNA-binding site, since VR and TR do not simultaneously bind to TEP1–RBD. RNase H digests of extracts containing VR annealed to complementary DNA oligonucleotides (ODNs) were synthesized in order to identify single-stranded regions of VR. These experiments suggest that the central loop of partially purified endogenous VR forms a more open and single-stranded structure than predicted by thermodynamic models. Combined with the results of our

VR mutations, these results suggest that the central loop of VR is important for its interaction with TEP1. Finally, by purifying recombinant vaults generated by co-infecting Sf9 insect cells with baculoviruses expressing MVP and a series of TEP1 truncations, we show that the p80 homology region of TEP1 also contains the vault-interaction domain.

MATERIALS AND METHODS

Yeast three-hybrid analysis

Mouse TEP1 deletions were generated by PCR, cloned into the pACT II yeast expression vector and confirmed by sequence analysis. PCR primers were engineered to contain an NcoI site for cloning purposes and are as follows. Forward primers for the following TEP1 amino acid sequences 1–871, 1–740 and 1–580: 5′-AATCCATGGCTATGGAGAAGCTCTGTGGGCATG-3′; 201–871: 5′-AATCCATGGCTCAAGAAGAAGAAAGCAC-AGAAG-3′; 270–871: 5′-AATCCATGGCTTCTGACCTTA-CCCGGGCATC-3′; and 400–871: 5′AATCCATGGCTCG-CCCTCAAAAGACAGAACG-3′. Reverse primers: 1–871, 201–871, 270–871 and 400–871: 5′-AATCCATGGTATGG TATCTAGTTGTCCC-3′; 1–740: 5′-AAT CCATGCGGTGT-CTTCACAAATCCTCC-3′; and 1–580: 5′-AATCCATGATC-GATAGAGTCATGAGC-3′. Mouse VR was cloned by PCR into the SmaI site of pIII/MS2-1 in sense and antisense orientations using the following primers: forward, 5′-CTGA-CCCGGGCCAGCTTTAGCTCAGC-3′; reverse, 5′-TTGAC-CCGGGAAAGGGCCAGGGAGCGCC-3′. Murine TR clones for use in the yeast three-hybrid system have been published previously (16). Plasmids were transformed into the L40i yeast strain and tested for TEP1–VR and TEP1–TR interactions as described previously (13,16,28).

TEP1–RBD expression and partial purification

The DNA sequence for amino acids 201–871 of murine TEP1 was PCR amplified and cloned into pET28a using forward and reverse primers containing engineered SalI and NotI sites, respectively, thus fusing the His-T7 tag onto the N-terminus of TEP1–RBD. Forward primer, 5′-ATCTGT-CGACAAGAAGAAGAAAGCACAGA AG-3′; reverse primer, 5′-ATAAGAATGCGGCCGCTTATAGTTTATCTA-GTTGTCCC-3′. The plasmid was sequenced and transformed into BL21 CodonPlus DE3 *E.coli* (Stratagene). A 500 ml culture was induced with 1 mM Isopropyl-β-D-thiogalactopyranoside for 2.5 h at 21°C, and lysed in 50 mM NaH_2PO_4, pH 8, 300 mM NaCl, 0.5% v/v Triton X-100, 10 μg/ml leupeptin by a 1 h incubation with 1 mg/ml lysozyme at 4°C followed by sonication (two 10 s pulses at setting 3.5). Cleared lysates were applied to a Ni-NTA column (Novagen) and washed according to the manufacturer's protocol with the final wash and elution containing 100 and 250 mM imidazole, respectively. The eluate was dialyzed into 20 mM Tris, pH 8, 150 mM NaCl, 1 mM $MgCl_2$, 10% glycerol and 1 mM DTT, and stored at −80°C.

Mutagenesis, EMSA and immunoprecipitation

VR and TR were PCR amplified using a forward primer engineered to incorporate a T7 promoter sequence to drive transcription and cloned into pUC 118. Point mutants were generated using the Quickchange Mutagenesis Kit (Stratagene), or by a second round of PCR using a transcription template (see below) using a forward or reverse primer incorporating the appropriate nucleotide alteration. Transcription reactions were performed using sequenced VR or TR PCR product templates derived from pUC 118 clones to ensure correct termination of transcription. EMSA was performed as described previously (24) with the following exception: 5 fmol of ^{32}P-CTP radiolabeled RNA was used in each binding reaction and native gels were electrophoresed at 300 V in 0.5× TBE for 1 and 4 h for VR and TR probes, respectively. Competitions were carried out by pre-incubating unlabeled RNA with TEP1–RBD for 10 min prior to the addition of radiolabeled RNA. Dried gels were exposed to PhosphorImager screens and imaged using the Typhoon 9410 (Molecular Dynamics). Immunoprecipitation of mTR/TEP1–RBD complexes was carried out by transferring the binding reaction into 90 μl 1× binding buffer containing 0.1 mg/ml BSA, followed by incubation with 1 μg antibody on ice for 40 min. Fifteen μl Protein A beads were then used to capture the complex by tumbling the tubes for 20 min at 4°C. The beads were washed three times with ice-cold binding buffer and boiled in SDS sample buffer.

RNase H digests

RNase H assays were performed on either P100 extract (RNP) or deproteinized P100 extract (RNA) prepared from either rat fibroblasts or HeLa cells. Antisense ODNs that span almost the entire length of rat VR or human VR1 were synthesized on an Applied Biosystems DNA synthesizer. Ten micrograms of total protein (P100) or deproteinized P100 (RNA), 0.5 μg of antisense ODNs and 0.4 U of RNase H (in a final volume of 25 μl) were incubated at 30°C for 1 h. Reactions were phenol:chloroform extracted, and ethanol precipitated in the presence of 10 μg of carrier tRNA and analyzed by northern blotting as described previously (8).

Baculoviruses, SF9 insect cell infections and vault purifications

The rat MVP-encoding baculovirus and human TEP1-encoding baculovirus have been described previously (4,29). DNA encoding human TEP1 amino acids 1–1650 and 1–125 were generated by PCR, cloned into pFastBac 1 and verified by sequencing. The primers used were as follows. The 1–1650 and 1–125 constructs were both made using the forward primer: 5′-CTACGTCGACCACCATGGAAAAACTCCAT-GGGCATG-3′. The reverse primer sequence for the 1–1650 clone encodes a C-terminal T7 epitope tag and is 5′-GCTT-TCTAGACTAACCCATTTGCTGTCCACCAGTCATGCTA-GCCATGAGGTGCCATCTCCGGGAGAG. The reverse primer sequence for the 1–125 clone also encodes a C-terminal T7 epitope tag and is 5′-GCTTTCTAGACTAACCCATTTGC-TGTCCACCAGTCATGCTAGCCATGCTGGCAGACAC-AGTGCTCTTTAG-3′. SalI and XbaI sites engineered into the primers were used to clone the PCR product into pFastBac (Invitrogen). A fragment of the hTEP1 cDNA, spanning the first 911 amino acids, was subcloned into pFastBac1 and engineered with an N-terminal tandem c-myc epitope tag (residues 408–439 of the human c-myc protein) and a C-terminal 6 histidine tag. The final insert sequence was confirmed using

fluorescent dideoxy-nucleotide sequencing and automated detection (ABI/PerkinElmer). The resulting 956 amino acid fusion protein has a predicted weight of 108.4 kDa. Viruses were generated according to the protocol of the Bac-to-Bac system (Invitrogen). Sf9 cells were maintained and infected with baculovirus(es) as described previously (4). Recombinant vaults were purified from infected Sf9 cell lysates and analyzed by western blot as described previously (4).

RESULTS

The entire Tetrahymena p80 homology region of murine TEP1 is required for the interaction with vault and telomerase RNAs

A truncation consisting of the first 871 amino acids of murine TEP1 has been previously shown to interact with mouse TR and multiple human VRs using a yeast three-hybrid assay (13,16). Briefly, this assay fuses an RNA of interest to the MS2 phage hairpin RNA, which binds to the MS2 coat protein, and can be used to test RNA–protein interactions by driving transcription of a reporter gene in a manner analogous to yeast two-hybrid assays (28). In addition to the p80 region, this 871 amino acid sequence contains four N-terminal 30 amino acid repeats of unknown significance. Since the region of homology between TEP1 and p80 is poorly conserved with other RNA-binding proteins at key residues (30), we decided to test a series of TEP1 truncations for two reasons: first, to determine whether it was possible to separate the RNA-binding activities for VR and TR, which might suggest a functional connection between the two RNAs; and second, if this was not possible, to further define the region of TEP1 critical for binding RNA. TEP1 deletions were made using the 1–871 amino acid region as a starting point (Figure 1A), and these constructs were transformed into the L40i yeast strain, along with plasmids expressing mTR and mVR sense and control, antisense RNAs fused to the MS2 hairpin RNA. An interaction between protein and RNA activates the *His3* reporter gene and allows the growth of yeast on media lacking histidine and containing 3-aminotriazole. Both the 1–871 amino acid construct and a construct lacking the 4 N-terminal repeats of TEP1 (amino acids 201–871) were able to bind to both TR and VR in sense but not antisense orientations based on this assay (Figure 1A, constructs 1 and 2; Figure 1B, 1s, 1as, 2s and 2as). Deletion of any sequences in the TEP1-p80 homology region resulted in the loss of RNA-binding ability of both TR and VR (Figure 1A, constructs 3–6 and Figure 1B, 3–6). Western blots of transformed yeast cultures verified that all of the TEP1 deletions were expressed (data not shown), although a substantial portion of construct 3 (amino acids 270–871) is found as a smaller breakdown product in yeast lysates. Thus, the entire p80 homology region (amino acids 201–871) is required for TEP1 to bind both VR and TR in an indirect yeast three-hybrid system; henceforth this domain will be referred to as TEP1–RBD.

Partially purified TEP1–RBD binds TR *in vitro*

Evidence exists that VR and TR bind to TEP1 *in vitro* and *in vivo*, but it has not yet been shown that TEP1 binds to these RNAs directly (13,16,22). Therefore, we expressed and purified from *E.coli* the murine TEP1–RBD fused to the HisT7 N-terminal epitope tag derived from pET28 (see Materials and Methods). We were unable to completely purify the recombinant protein away from contaminating bacterial proteins without washing TEP1–RBD off the Ni-NTA resin. Nevertheless, we were able to partially purify enough recombinant TEP1–RBD (Figure 2A) to determine whether it could interact with RNA *in vitro* using EMSA. Although full-length mTR binds to TEP1–RBD using EMSA (data not shown), we also transcribed mTR nt 1–223, which is sufficient to interact with TEP1 in the yeast three-hybrid assay (A. Reda and L. Harrington, unpublished data), rather than full-length mTR, to facilitate resolution of the RNA and RNP complexes on native gels. Incubation with increasing amounts of TEP1–RBD induced a small shift in the mobility of the 223 nt mTR probe using EMSA (Figure 2B, lanes 1–4), and this association was competed with pre-incubation of 50× unlabeled full-length TR (Figure 2B, lane 5). Surprisingly, even 250× excess unlabeled mVR was unable to compete with the TR probe for binding to TEP1–RBD (Figure 2B, lane 6), but an mVR variant (see below) did compete with TR probe, although less effectively than TR itself (Figure 2B, compare lanes 7–8 with lane 5). Using more than 80 ng TEP1–RBD in the binding reactions did not result in increased TR binding, nor did using more than 50-fold molar excess of unlabeled TR result in much additional competition with labeled probe (data not shown), indicating that the majority of the RNA is unable to bind despite a high molar excess of protein to target RNA. To test the specificity of RNA binding by TEP1, four non-specific competitor RNAs were used; three RNAs were unable to compete for binding to TEP1 even at 500× excess (Figure 2B, lanes 9–11). The NL15 RNA is an artificial RNA with both single- and double-stranded regions that interacts with the La protein *in vivo*, but does not bind in a 3′ uridylate dependent manner (31). La has previously been shown to interact with the VR and the TR (24,32,33). As La also interacts with the vault particle, this seemed to be a relevant RNA to test for binding to TEP1–RBD (24). However, *in vitro* transcription of the multiple-cloning site of linearized pBluescript SK+ containing the T7 promoter yielded an RNA, which was able to efficiently compete with TR for binding at 50-fold molar excess (Figure 2B, lane 12). This indicates that TEP1–RBD, like its *Tetrahymena* p80 homolog, has limited specificity with respect to its affinity for RNA *in vitro* (19). The specificity of the RNA–protein complex was then further analyzed since the TEP1–RBD protein was only partially purified. We used a monoclonal antibody directed against the T7 epitope tag of the recombinant TEP1–RBD protein to co-immunoprecipitate the mTR (nt 1–223) probe (Figure 2C, lanes 1 and 2). Control antibodies (Figure 2C, lanes 3–6) did not bring down either the TEP1–RBD protein or the mTR RNA, demonstrating that the band shift seen using EMSA was specifically due to binding to TEP1–RBD.

A VR variant has an enhanced ability to bind TEP1–RBD *in vitro*

Since unlabeled mVR could not compete with TR for binding to TEP1–RBD *in vitro*, we repeated the EMSAs using radiolabeled VR transcripts. When labeled mVR was

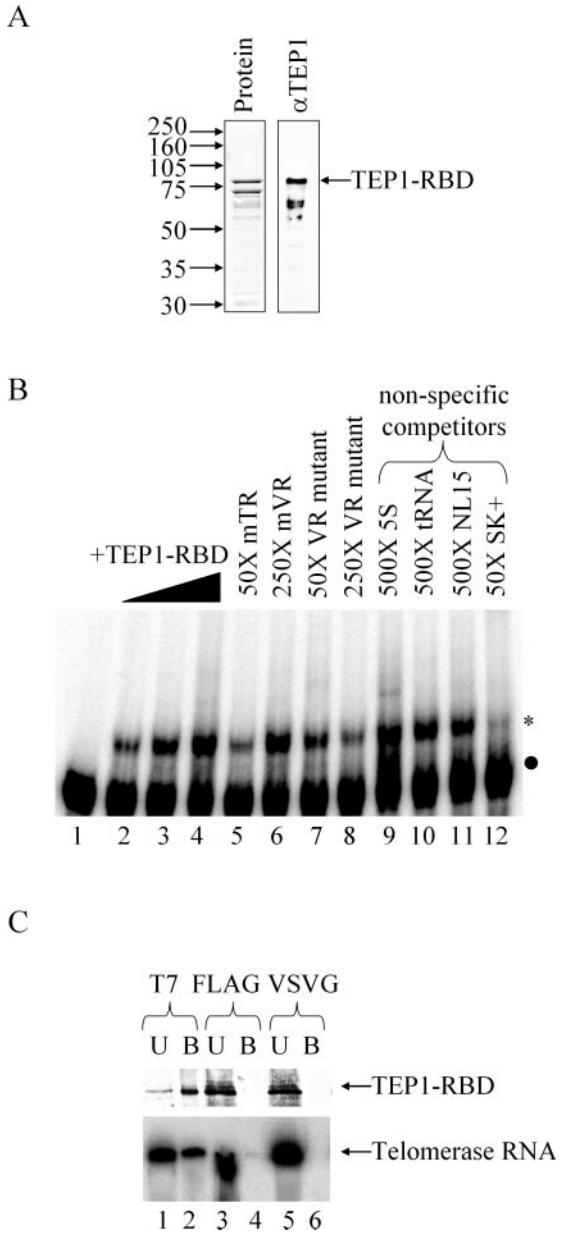

Figure 2. Partially purified murine TEP1–RBD interacts with TR *in vitro* but has limited specificity. (**A**) Amino acids 201–871 of murine TEP1 were expressed in *E.coli* and partially purified using the hexahistidine tag derived from the pET28a vector. Shown are a Coomassie-stained gel (left panel) and western blot (right panel) using anti-TEP1 polyclonal antibodies. (**B**) EMSA of nt 1–223 of mouse TR incubated with TEP1–RBD. Five fmol ^{32}P-labeled probe was incubated with 0, 5, 20 and 80 ng TEP1–RBD (lanes 1–4). Probe was competed off with 50× full-length TR (lane 5) and increasing amounts of mVR double point mutant (lanes 7 and 8), but not wild-type mVR (lane 6). The 250× unlabeled 5S Ribosomal RNA, tRNA^{phe} or an artificial RNA (NL15) do not compete with the probe (lanes 7–9), but 50× excess of an artificial RNA derived from the pBluescript polylinker region does compete efficiently (lane 10). Labeled RNA is indicated with a black dot and shifted complexes are indicated with an asterisk. (**C**) Immunoprecipitation of TEP1–RBD from binding reactions using anti-T7 monoclonal antibody co-immunoprecipitates the TR transcript. Equivalent amounts of the bound (B) and unbound (U) fraction were analyzed by either western blot using anti-TEP1 polyclonal antibody (upper panel) or by fractionation on a 10% acrylamide/8 M urea gel (lower panel). The latter gel was dried and radioactive bands visualized by phosphorimager analysis. Antibodies to the T7 epitope (lanes 1 and 2), but not antibodies to the FLAG (lanes 3 and 4) and VSVG (lanes 5 and 6) epitopes, immunoprecipitated both TEP1–RBD and TR.

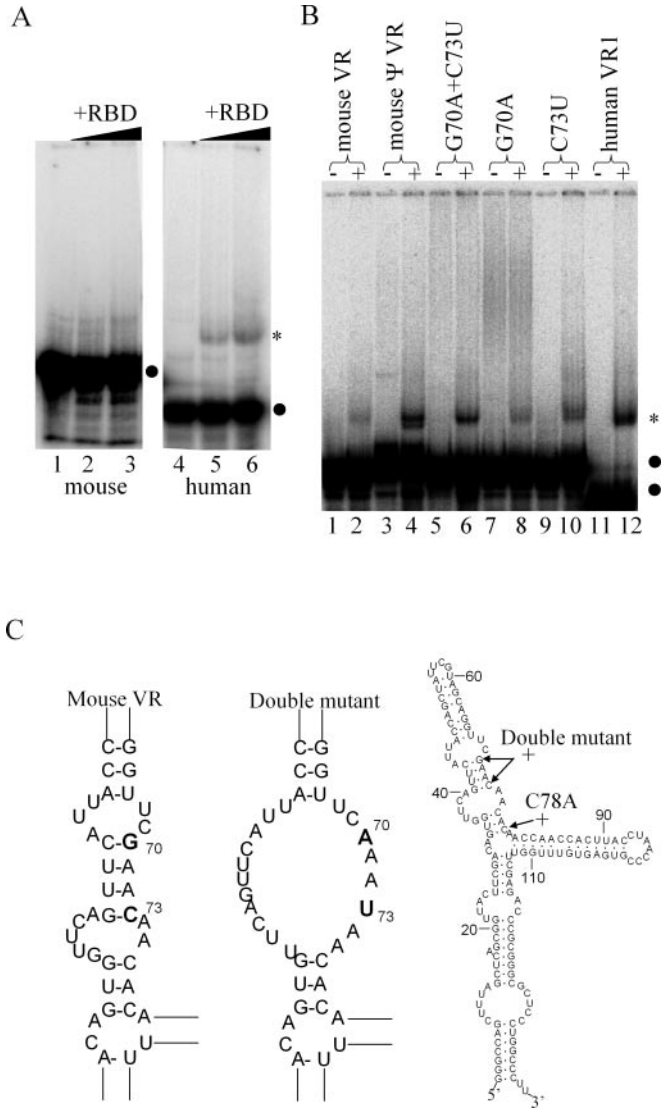

Figure 3. Mutagenesis of murine VR enhances its binding to TEP1–RBD. (**A**) EMSA of VR–TEP1–RBD complexes. Binding reactions contained 5 fmol of ^{32}P-labeled murine VR (left panel) or human VR1 (right panel) incubated with 0 (lanes 1 and 4), 20 (lanes 2 and 5) and 80 (lanes 3 and 6) ng of TEP1–RBD. (**B**) EMSA of VR probes (5 fmol) without (−) or with (+) 80 ng TEP1–RBD in the binding reaction. Wild-type mouse VR interacts poorly or not at all with TEP1–RBD (lanes 1 and 2), but a highly related sequence in the mouse genome that is not expressed binds more strongly (lanes 3 and 4). A VR double point mutant G70A, C73U (lanes 5 and 6) binds more strongly to TEP1–RBD. Also shown are the corresponding single mutants in mouse VR (lanes 7–10) and human VR1 (lanes 11 and 12). Labeled RNAs are indicated with a black dot and shifted complexes are indicated with an asterisk. (**C**) The thermodynamically predicted secondary structure of the wild-type (left structure) and double point mutant (center structure) mouse VR, focusing on the regions of interest only. Also shown is the entire predicted structure of mouse VR, along with the position of the double point mutant and the C78 to A mutation, which has enhanced binding.

incubated with TEP1–RBD, no RNP complex was observed, as might be expected from the inability of mVR to compete with labeled mTR for binding to TEP1–RBD (Figure 3A, left panel). In contrast, when we used the related human hVR1, we detected a low-level interaction with the murine TEP1–RBD using EMSA (Figure 3A, right panel). We recently reported that the mouse genome contains two VR genes, *mvg1* and

Table 1. Stepwise reversion of ΨmVR to mVR sequence

Nucleotide	ΨmVR	1	2	3	4	5	6	mVR
16	G	G	G	**C**	**C**	**C**	**C**	**C**
28	U	U	**C**	**C**	**C**	**C**	**C**	**C**
36	U	U	**G**	**G**	**G**	**G**	**G**	**G**
70	A	A	A	A	A	A	**G**	**G**
73	U	U	U	U	U	**C**	U	**C**
91	G	G	G	G	**A**	**A**	**A**	**A**
100	A	A	A	A	**G**	**G**	**G**	**G**
121	G	**C**	**C**	**C**	**C**	**C**	**C**	**C**
Binding	+	+	+	+	+	±	±	−

The position of the 8 nt differences between the two RNAs are shown in the leftmost column, and the base found in ΨmVR and mVR at each is indicated. Columns 1–6 are variant VRs tested for binding to TEP1–RBD, with the result shown in the bottom row.

mvg2; however, only *mvg1* is expressed (25). The second, a pseudogene, was the only murine VR clone identified from our original genomic screen for VR sequences and was initially presumed to be the one and only VR gene. This VR pseudogene (henceforth termed ΨmVR) contains only 8 nt changes as compared with mVR, and is predicted to form into the evolutionarily conserved VR structure. Thus, we had initially expressed the ΨmVR 'coding region' *in vitro* using a T7 promoter and determined that this VR pseudotranscript is also able to interact with TEP1–RBD in mobility shifts (Figure 3B, lane 4).

This observation provided a starting point for a mutational analysis strategy to determine why mVR was unable to bind to TEP1–RBD *in vitro*. ΨmVR sequences were replaced with mVR sequences in a stepwise manner (Table 1) and assayed for the loss of binding to TEP1 using EMSA. The first column of Table 1 indicates the position of the 8 nt differences between ΨmVR and mVR, and subsequent columns indicate intermediate mVR sequences after nucleotides were altered to revert to the mVR sequence 1 or 2 nt at a time. We were able to revert the ΨmVR sequence back to the mVR sequence without losing binding to TEP1–RBD until reversion was attempted at either nt 70 or 73. Once the key residues responsible for ΨmVR's interaction with TEP1–RBD were identified, these residues were altered in mVR, and it was confirmed using EMSA that this mVR double mutant is able to interact with TEP1–RBD (Figure 3B, compare lanes 4, 6 and 12). The double mutant alters the base pairing from Watson–Crick to wobble, and is predicted to open a loop in this region of the VR (Figure 3C, left and center structures) using the mfold RNA structure prediction program (34). Because this structure borders the conserved central loop of VR (defined as the region where all three arms of the VR converge in the nine different VR sequences identified across the various species to date), we hypothesized that mutations opening up the central loop might also increase TEP1 binding. Novel mutations in unmodified mVR, which might weaken the stability of the helix adjacent to the central loop without grossly altering the predicted structure of VR, were synthesized. One mutation, C78→A, showed enhanced binding to TEP1–RBD similar to the mVR double mutant (data not shown) (results summarized in Figure 3C, right structure).

The specificity of the interaction between the mVR double mutant and TEP1–RBD was tested using a number of

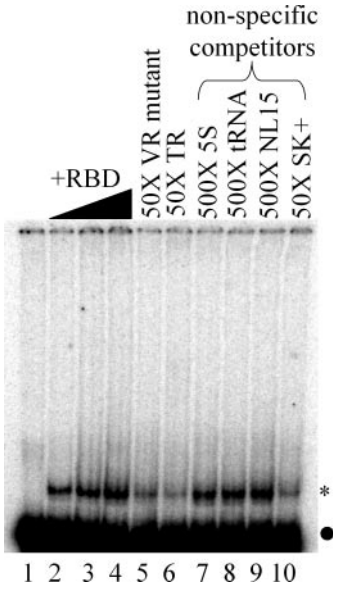

Figure 4. The mVR point mutant competes with TR for binding to TEP1–RBD. EMSA of mVR double point mutant incubated with 0, 5, 20 and 80 ng of TEP1–RBD (lanes 1–4). Unlabeled mVR mutant or mouse TR (50×) competes with the labeled probe (lanes 5 and 6). Three irrelevant RNAs do not compete with TR for binding to TEP1–RBD (lanes 7–9), but the pBluescript transcript does compete efficiently (lane 10) as in Figure 2. Labeled RNA is indicated with a black dot and shifted complexes are indicated with an asterisk.

unlabeled competitor RNAs. Addition of increasing amounts of TEP1–RBD to the mobility shift binding reactions resulted in an increasingly intense band representing the mVR double mutant–protein complex (Figure 4, lanes 1–4). Pre-incubation with 50× excess of the unlabeled VR double mutant competed most of mobility shift, as did 50× excess TR (Figure 4, lanes 5 and 6). However, not all of the labeled RNA could be competed, similar to TR competition results (Figure 2B). This VR/TR competition for binding to TEP1–RBD indicates that it is likely that either VR or TR, but not both simultaneously, is able to bind to TEP1. Increasing the amount of TEP1–RBD to more than 80 ng did not result in increased VR binding, nor did incubation with more than 50× unlabeled VR double mutant result in additional competition with labeled probe (data not shown). The same four non-specific competitor RNAs were used as with labeled TR, with identical results; again only the SK+ transcript was able to compete for binding (Figure 4, lanes 7–10). Addition of the anti-T7 monoclonal antibody to the binding reaction also resulted in a faint supershift on EMSA (data not shown).

RNase H mapping of VR indicates that regions surrounding the central loop are single stranded

We hypothesized that *in vivo* the central loop of the VR may be in a more open conformation that may facilitate TEP1 binding. To determine whether sequences in the central loop of the VR were available for base pairing, we used an oligodeoxynucleotide-directed RNase H cleavage assay (35). We undertook a preliminary analysis of the secondary structure of both rat VR (Figure 5, left panels), which is highly related to murine VR, and human VR1 (Figure 5, right panels) using this assay. Vault-associated VR was obtained from

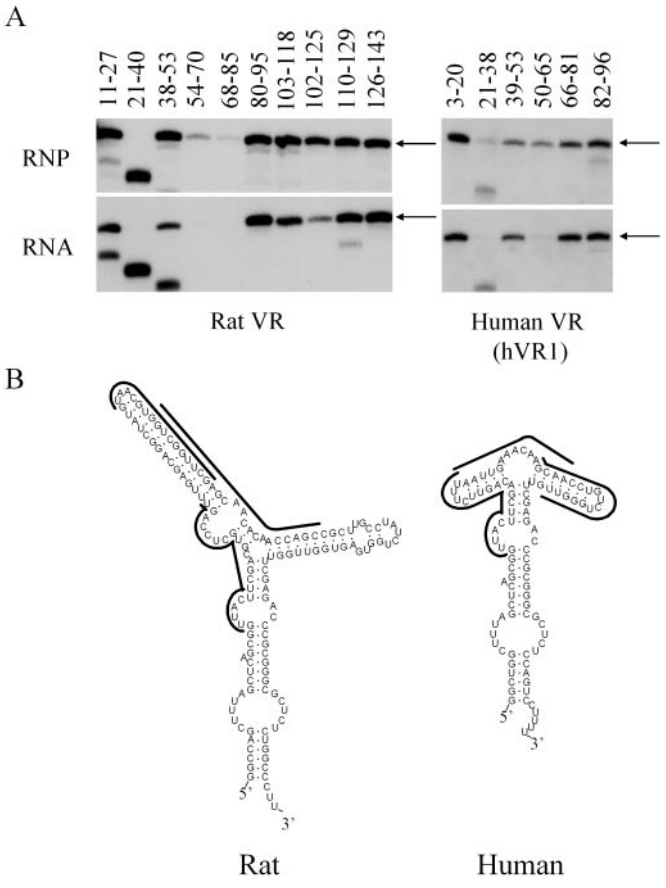

Figure 5. RNase H digests of vault-bound and deproteinated VR. (**A**) Oligodeoxynucleotide-directed RNase H cleavage of the VR. P100 extract (RNP) or deproteinized P100 (RNA) purified from rat fibroblasts (left panel) or HeLa cells (right panel) was incubated with the indicated antisense ODN and RNase H. RNA was extracted from each sample and fractionated on a 10% denaturing polyacrylamide gel. The gel was electroblotted to a Zeta GT+ membrane and probed with the randomly primed VR gene. Intact VR is indicated by the arrow, and lower bands represent cleaved VR. (**B**) Thermodynamic prediction of rat VR and human VR1 secondary structures. The lines indicate regions of single-stranded RNA based upon RNase H digests of vault-associated VR.

resuspended high speed (100 000 *g*) pellets and deproteinated VR obtained from phenol:chloroform extraction of these resuspended pellets. A series of overlapping ODNs complementary to the VRs were each annealed to VR from either rat fibroblast or HeLa cell lysates for rat and human VRs, respectively. RNase H was then added to cleave RNA–DNA hybrids, which form in regions where RNA secondary structure is largely single stranded (35). The extent of cleavage of the 141 nt rat VR was analyzed by northern blotting (Figure 5A). In the absence of VR-associated vault proteins, three ODNs, 21–40, 54–70 and 68–85, directed nearly complete cleavage of rat VR (Figure 5A, lower left panel, RNA). In addition, antisense ODNs 11–27, 38–53 and 102–125 also led to varying amounts of digestion of the VR, whereas the remaining four ODNs (80–95, 103–118, 110–129 and 126–143) had either no effect or directed <5% cleavage of the VR. When vault proteins remain associated with VR, a similar pattern of cleavage is seen by ODNs 21–40, 54–70 and 68–85 (Figure 5A, upper left panel, RNP), whereas the remaining seven ODNs were presumably unable to hybridize with VR, as only minimal cleavage of the VR was observed. These results suggest that bases 21–40 and 54–85 are in an open conformation available for base pairing in the VR whether or not protein is associated. These data are inconsistent with the predicted secondary structure of the rat VR, which indicates that bases 25–85 are base paired in a stem–loop structure (Figure 5B, left panel) (11). Similar results were obtained using ODN-directed cleavage of the 98 nt human VR (hVR1). In the absence of VR-associated vault proteins, ODNs 21–38 and 50–65 directed complete cleavage of hVR1, and ODN 39–53 led to partial cleavage (Figure 5A, lower right panel, RNA). In the presence of vault proteins, these three ODNs again led to the most substantial cleavage of VR. According to these data, both rat and human VR have a significantly more open structure *in vivo* in the regions surrounding the central loop than was predicted by thermodynamic models (Figure 5B, left and right panels). We found minor differences between protein-bound and deproteinated RNA, but overall the rat and human VRs were found to be single stranded in regions of VR that are poorly conserved in sequence across species. That may indicate that it is the structure and not the sequence *per se* that is important for TEP1–RBD binding.

The p80 region of TEP1 also binds vaults

Although TEP1 did not interact with either MVP or VPARP in a yeast two-hybrid assay (36), TEP1 does interact directly with MVP, as co-infection of baculoviruses expressing TEP1 and MVP generates vault-like particles in insect cells that, when purified, contain TEP1 (29). Thus, TEP1 may be able to interact with intact vault particles but not MVP monomers. In order to identify a TEP1–MVP interaction domain, we generated a series of TEP1 truncations for use in the baculovirus expression system (Figure 6A). Baculoviruses expressing the various TEP1 truncations were then used to infect Sf9 insect cell cultures, either alone or in combination with an MVP-expressing baculovirus. Vaults were purified from the co-infected cells as described previously (4). As a final purification step, fractions enriched in recombinant vaults are layered over a 10–60% discontinuous sucrose gradient; vaults comprising HisT7-epitope tagged MVP subunits were used in this study. These particles fractionate predominantly in the 45% sucrose layer (Figure 6B, 'MVP' panel). When TEP1 truncations were expressed without MVP, the vault purification scheme removed each truncation prior to the sucrose gradient step [Figure 6B, 1–3, upper (−) panels]. When expressed together with MVP [Figure 6B, 1–3, lower (+) panels], some TEP1 truncations were seen to co-purify with the recombinant vaults [Figure 6B, 1–3, lower (+) panels]. Truncations consisting of amino acids 1–1650 and 1–911 (Figure 6A, constructs 1 and 2; Figure 6B, panels 1 and 2) each co-purified with vaults, whereas a truncation consisting of amino acids 1–125, which contains the 4 N-terminal repeats, failed to interact (Figure 6A, construct 3 and Figure 6B, panel 3). By deduction, amino acids 126–911 contain a vault-interaction domain. A fourth TEP1 construct, consisting of amino acids 201–1650 of murine TEP1, also interacted with vaults even though it was poorly expressed in insect cells, possibly due to the deletion of the TEP1 N-terminus (data not shown). Therefore, the p80 region of TEP1

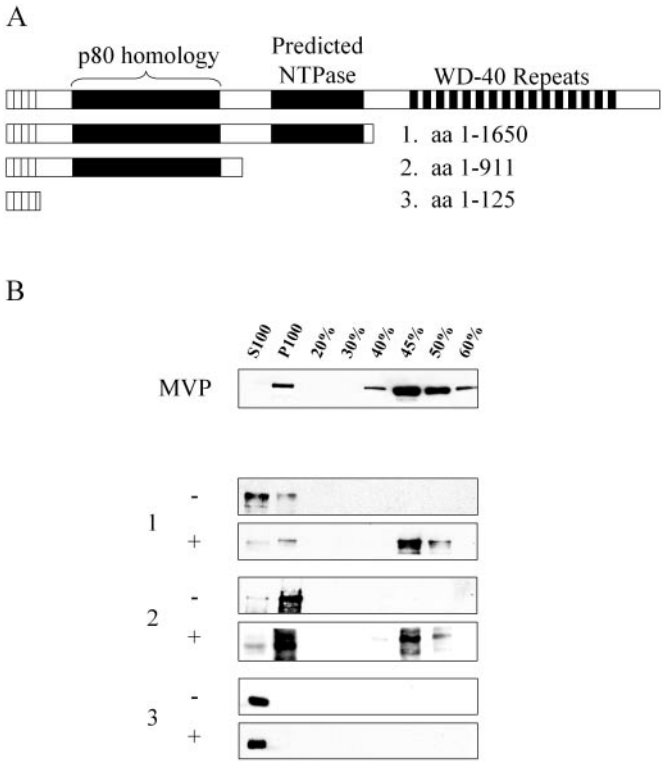

Figure 6. The p80 homology region of TEP1 contains the vault interaction domain. (**A**) TEP1 truncations were co-expressed with the MVP in Sf9 insect cells using a baculovirus expression vector. (**B**) MVP forms vaults when expressed in insect cells, which are found entirely in the high-speed pellet (P100) of cell lysates and can be purified to near-homogeneity. Vault-interacting proteins will co-purify with vaults. Vaults were further enriched, and as a final step, samples were loaded onto a 20–60% sucrose gradient and centrifuged for 16 h. Sucrose fractions were pelleted, resuspended in 20 mM MES buffer, pH 6.5 and analyzed by western blot. Vaults fractionate largely in the 45% sucrose layer (upper panel). In the absence (−) of MVP-baculovirus co-infection, TEP1 truncations fractionate in either the high-speed supernatant (S100), P100, or both, and are lost in the purification scheme before the sucrose gradient step (1, 2, and 3, upper panels). When MVP is present (+), TEP1 truncations able to interact with vaults are found largely in the 45% sucrose layer (column 1, 2, and 3, lower panels).

(amino acids 201–911) appears to contain both the RNA-binding and vault-interaction domains. The VR is not present in the baculovirus expression system, and *Sf9* insect cells do not contain endogenous vault components, so the TEP1–vault interaction is not mediated by VR. The mapping of a vault-interaction domain to this conserved region suggests the intriguing possibility that *Tetrahymena* might contain vaults or a protein conferring a related function. A database search of the *Tetrahymena* genome did not identify an MVP homolog, although assembly of the sequences for this genome is not yet complete (The Institute for Genomic Research website at http://www.tigr.org).

DISCUSSION

PSI-blast searches using the amino acid sequence of p80 have previously identified two conserved regions that together span the entire length of the protein. First, the TROVE (Telomerase, Ro and Vault) module was identified as an evolutionarily conserved (presumed) multi-domain region found in TEP1, p80, Ro60 and a number of uncharacterized bacterial proteins (30). This region spans amino acids 227–685 of murine TEP1. Ro60 binds to small RNAs termed 'Y RNAs' along with the La autoantigen in a small RNP complex and has been proposed to contain an RNA recognition motif (RRM domain) based upon the presence of RNP-1 and RNP-2 motifs that are the hallmark of this domain (37,38). However, putative RRMs in p80 and TEP1 have an unusually short spacing of the RNP-1 and RNP-2 motifs and contain conserved polar residues in regions that are non-polar in other RRMs (30). The second domain found using databases searches of p80 is a von Willebrand type A (vWA) domain, which can be involved in a number of functions such as binding to metals, or mediating protein–protein interactions, often in extracellular proteins or in multiprotein complexes (39). This domain is also found adjacent to the TROVE module in TEP1, and corresponds to amino acids 678–861 (29). Interestingly, a vWA domain is found in VPARP as well (30). Our study indicates that an intact TROVE module is required for RNA-binding activity, but we were unable to remove the vWA sequences from the p80 homology region of TEP1 in our yeast three-hybrid assay without interfering with the ability of TEP1 to bind RNA. Since vWA domains are not known to bind RNA, it is possible that the removal of this region disrupts the conformation of the RNA-binding domain in the TROVE module. An analysis of Ro60 similarly determined that even small amino acid deletions in the protein led to the loss of binding to Y RNAs, so it appears that this aspect of the two proteins has also been conserved (40). As we have also mapped the vault-interaction domain of TEP1 to the p80 homology region, either the TROVE module or the vWA domain must mediate this interaction. TEP1 interacts directly with MVP in the insect cell expression system, and is not dependent upon VR for its association with vaults (29). Thus, it is not clear what mechanism targets VR but not TR into the vault particle. One possibility is that since the RNA-binding and vault-binding regions of TEP1 are either in close proximity or overlap, binding of TR to TEP1 could interfere with the ability of the protein to complex with vaults, while binding of VR to TEP1 could promote the TEP1–vault interaction. However, the effect of VR or TR on the stability of the TEP1–vault association is difficult to assess using the insect cell expression system, since the vault purification scheme incorporates an RNase treatment step to remove ribosomes.

Since both VPARP and TEP1 associate with vaults and telomerase (16,17,23), it is possible that there is a functional connection between the two RNPs. The present study indicates that VR or TR, but not both, can interact with a given TEP1 molecule, so it does not seem that VR could directly associate with the telomerase complex via TEP1 without displacing TR. Likewise, neither telomerase activity nor telomerase RNA has been found associated with purified rat liver vaults or vaults immunoprecipitated from tissue culture cells, respectively, so it does not appear likely that either RNA is to be found in the other RNP complex (13,26). The results of our RNase H experiments suggest that the *in vivo* structure of the VR diverges significantly from structure predictions based upon thermodynamic models. Specifically, the left and right arms of VR, which are essentially the only regions of the RNA that are not conserved across species or even within a single species

when multiple VRs are present, are largely single stranded. The central loop of purified endogenous VR is, therefore, considerably larger than seems thermodynamically likely, which may be due to binding of TEP1 to the conserved lower region of the loop. It also seems likely that the *in vitro* transcribed VR used in EMSA might fold into a structure resembling the more thermodynamically favorable predicted structures shown in Figure 5, rather than a structure containing large stretches of single-stranded RNA. This would explain why only a small fraction of the RNA interacts with TEP1–RBD *in vitro*. Mutations in VR that disrupt base pairing near the VR central loop enhance binding to TEP1 *in vitro*, which suggests that this could be the case, and that these mutations might partially compensate for the absence of factors promoting the TEP1–VR interaction *in vivo*. Such missing factors could include MVP, VPARP and, in particular, the La RNA-binding protein, which binds VR stably apart from the vault particle and loosely purifies with vaults, suggesting that it may promote the VR–TEP1 interaction in vaults. Additionally, the full-length TEP1 contains a putative NTPase motif, which could potentially regulate the association of TEP1 with VR. Thus far, we have been unable to purify sufficient quantities of recombinant TEP1 containing both the p80 and putative NTPase regions to test this hypothesis, since TEP1 is particularly susceptible to degradation when expressed in insect cells. Finally, it is difficult to rule out misfolding of either RNA or the TEP1–RBD protein when conducting *in vitro* experiments using purified components, either of which could affect the specificity and stability of the RNA–protein interaction.

It was surprising that wild-type mouse VR did not readily interact with TEP1–RBD, since human VR1, mutant mVR, TR and a non-specific RNA did interact. Genetic evidence has demonstrated that TEP1 directs VR to the vault particle and influences its stability *in vivo*. Therefore, this study suggests that additional components are probably required for TEP1 to bind specifically to RNA. The complexity of reconstituting the TEP1–VR interaction *in vitro* may explain why non-specific binding of some RNAs to TEP1 is observed in the current study, and also why studies of p80-TR binding also reported non-specific binding of RNA (19). Overall, these results indicate that binding of RNA to TEP1 may be regulated by other cellular factors and suggest that the RNA-binding properties of TEP1 *in vitro* are probably similar to those seen with p80.

ACKNOWLEDGEMENTS

This work was supported by grants from the G. Harold and Leila Y. Mathers Charitable Foundation (01124244 to L.H.R.), the National Science Foundation (MCB-0210690 to L.H.R.) and the NIH (AG16629-01 to L.H.). We thank the following members of the Harrington laboratory for their experimental contributions: Bryan Snow for construction of the 1–911 amino acid TEP1 baculovirus construct, Isabel Arruda for unpublished preliminary results in mapping the minimal TEP1–RBD in the yeast three-hybrid assay and Alexandra Reda for unpublished results that 1–223 nt mTR is sufficient to interact with mTep1 in the yeast three-hybrid assay. Funding to pay the Open Access publication charges for this article was provided by the G. Harold and Leila Y. Mathers Charitable Foundation.

REFERENCES

1. Kedersha,N.L. and Rome,L.H. (1986) Isolation and characterization of a novel ribonucleoprotein particle: large structures contain a single species of small RNA. *J. Cell. Biol.*, **103**, 699–709.
2. Kedersha,N.L., Miquel,M.C., Bittner,D. and Rome,L.H. (1990) Vaults. II. Ribonucleoprotein structures are highly conserved among higher and lower eukaryotes. *J. Cell. Biol.*, **110**, 895–901.
3. Kong,L.B., Siva,A.C., Rome,L.H. and Stewart,P.L. (1999) Structure of the vault, a ubiquitous cellular component. *Structure Fold. Des.*, **7**, 371–379.
4. Stephen,A.G., Raval-Fernandes,S., Huynh,T., Torres,M., Kickhoefer,V.A. and Rome,L.H. (2001) Assembly of vault-like particles in insect cells expressing only the major vault protein. *J. Biol. Chem.*, **276**, 23217–23220.
5. Chugani,D.C., Rome,L.H. and Kedersha,N.L. (1993) Evidence that vault ribonucleoprotein particles localize to the nuclear pore complex. *J. Cell. Sci.*, **106**, 23–29.
6. Hamill,D.R. and Suprenant,K.A. (1997) Characterization of the sea urchin major vault protein: a possible role for vault ribonucleoprotein particles in nucleocytoplasmic transport. *Dev. Biol.*, **190**, 117–128.
7. Scheffer,G.L., Wijngaard,P.L., Flens,M.J., Izquierdo,M.A., Slovak,M.L., Pinedo,H.M., Meijer,C.J., Clevers,H.C. and Scheper,R.J. (1995) The drug resistance-related protein LRP is the human major vault protein. *Nature Med.*, **1**, 578–582.
8. Kickhoefer,V.A., Rajavel,K.S., Scheffer,G.L., Dalton,W.S., Scheper,R.J. and Rome,L.H. (1998) Vaults are up-regulated in multidrug-resistant cancer cell lines. *J. Biol. Chem.*, **273**, 8971–8974.
9. Kolli,S., Zito,C.I., Mossink,M.H., Wiemer,E.A. and Bennett,A.M. (2004) The major vault protein is a novel substrate for the tyrosine phosphatase SHP-2 and scaffold protein in epidermal growth factor signaling. *J. Biol. Chem.*, **279**, 29374–29385.
10. Mossink,M.H., van Zon,A., Franzel-Luiten,E., Schoester,M., Kickhoefer,V.A., Scheffer,G.L., Scheper,R.J., Sonneveld,P. and Wiemer,E.A. (2002) Disruption of the murine major vault protein (MVP/LRP) gene does not induce hypersensitivity to cytostatics. *Cancer Res.*, **62**, 7298–7304.
11. Kickhoefer,V.A., Searles,R.P., Kedersha,N.L., Garber,M.E., Johnson,D.L. and Rome,L.H. (1993) Vault ribonucleoprotein particles from rat and bullfrog contain a related small RNA that is transcribed by RNA polymerase III. *J. Biol. Chem.*, **268**, 7868–7873.
12. Kickhoefer,V.A., Siva,A.C., Kedersha,N.L., Inman,E.M., Ruland,C., Streuli,M. and Rome,L.H. (1999) The 193-kD vault protein, VPARP, is a novel poly(ADP-ribose) polymerase. *J. Cell. Biol.*, **146**, 917–928.
13. Kickhoefer,V.A., Stephen,A.G., Harrington,L., Robinson,M.O. and Rome,L.H. (1999) Vaults and telomerase share a common subunit, TEP1. *J. Biol. Chem.*, **274**, 32712–32717.
14. Kong,L.B., Siva,A.C., Kickhoefer,V.A., Rome,L.H. and Stewart,P.L. (2000) RNA location and modeling of a WD40 repeat domain within the vault. *RNA*, **6**, 890–900.
15. Collins,K., Kobayashi,R. and Greider,C.W. (1995) Purification of Tetrahymena telomerase and cloning of genes encoding the two protein components of the enzyme. *Cell*, **81**, 677–686.
16. Harrington,L., McPhail,T., Mar,V., Zhou,W., Oulton,R., Bass,M.B., Arruda,I. and Robinson,M.O. (1997) A mammalian telomerase-associated protein. *Science*, **275**, 973–977.
17. Nakayama,J., Saito,M., Nakamura,H., Matsuura,A. and Ishikawa,F. (1997) TLP1: a gene encoding a protein component of mammalian telomerase is a novel member of WD repeats family. *Cell*, **88**, 875–884.
18. Miller,M.C. and Collins,K. (2000) The Tetrahymena p80/p95 complex is required for proper telomere length maintenance and micronuclear genome stability. *Mol. Cell*, **6**, 827–837.
19. Mason,D.X., Autexier,C. and Greider,C.W. (2001) Tetrahymena proteins p80 and p95 are not core telomerase components. *Proc. Natl Acad. Sci. USA*, **98**, 12368–12373.
20. Witkin,K.L. and Collins,K. (2004) Holoenzyme proteins required for the physiological assembly and activity of telomerase. *Genes Dev.*, **18**, 1107–1118.
21. Liu,Y., Snow,B.E., Hande,M.P., Baerlocher,G., Kickhoefer,V.A., Yeung,D., Wakeham,A., Itie,A., Siderovski,D.P., Lansdorp,P.M. *et al.* (2000) Telomerase-associated protein TEP1 is not essential for telomerase activity or telomere length maintenance *in vivo*. *Mol. Cell. Biol.*, **20**, 8178–8184.

22. Kickhoefer,V.A., Liu,Y., Kong,L.B., Snow,B.E., Stewart,P.L., Harrington,L. and Rome,L.H. (2001) The Telomerase/vault-associated protein TEP1 is required for vault RNA stability and its association with the vault particle. *J. Cell. Biol.*, **152**, 157–164.
23. Liu,Y., Snow,B.E., Kickhoefer,V.A., Erdmann,N., Zhou,W., Wakeham,A., Gomez,M., Rome,L.H. and Harrington,L. (2004) Vault poly(ADP-ribose) polymerase is associated with mammalian telomerase and is dispensable for telomerase function and vault structure *in vivo*. *Mol. Cell. Biol.*, **24**, 5314–5323.
24. Kickhoefer,V.A., Poderycki,M.J., Chan,E.K. and Rome,L.H. (2002) The La RNA-binding protein interacts with the vault RNA and is a vault-associated protein. *J. Biol. Chem.*, **277**, 41282–41286.
25. Kickhoefer,V.A., Emre,N., Stephen,A.G., Poderycki,M.J. and Rome,L.H. (2003) Identification of conserved vault RNA expression elements and a non-expressed mouse vault RNA gene. *Gene*, **309**, 65–70.
26. van Zon,A., Mossink,M.H., Schoester,M., Scheffer,G.L., Scheper,R.J., Sonneveld,P. and Wiemer,E.A. (2001) Multiple human vault RNAs. Expression and association with the vault complex. *J. Biol. Chem.*, **276**, 37715–37721.
27. Kedersha,N.L., Heuser,J.E., Chugani,D.C. and Rome,L.H. (1991) Vaults. III. Vault ribonucleoprotein particles open into flower-like structures with octagonal symmetry. *J. Cell. Biol.*, **112**, 225–235.
28. SenGupta,D.J., Zhang,B., Kraemer,B., Pochart,P., Fields,S. and Wickens,M. (1996) A three-hybrid system to detect RNA–protein interactions *in vivo*. *Proc. Natl Acad. Sci. USA*, **93**, 8496–8501.
29. Mikyas,Y., Makabi,M., Raval-Fernandes,S., Harrington,L., Kickhoefer,V.A., Rome,L.H. and Stewart,P.L. (2004) Cryoelectron microscopy imaging of recombinant and tissue derived vaults: localization of the MVP N termini and VPARP. *J. Mol. Biol.*, **344**, 91–105.
30. Bateman,A. and Kickhoefer,V. (2003) The TROVE module: a common element in Telomerase, Ro and Vault ribonucleoproteins. *BMC Bioinformatics*, **4**, 49.
31. Grimm,C., Lund,E. and Dahlberg,J.E. (1997) *In vivo* selection of RNAs that localize in the nucleus. *EMBO J.*, **16**, 793–806.
32. Seto,A.G., Zaug,A.J., Sobel,S.G., Wolin,S.L. and Cech,T.R. (1999) *Saccharomyces cerevisiae* telomerase is an Sm small nuclear ribonucleoprotein particle. *Nature*, **401**, 177–180.
33. Ford,L.P., Shay,J.W. and Wright,W.E. (2001) The La antigen associates with the human telomerase ribonucleoprotein and influences telomere length *in vivo*. *RNA*, **7**, 1068–1075.
34. Zuker,M. (2003) Mfold web server for nucleic acid folding and hybridization prediction. *Nucleic Acids Res.*, **31**, 3406–3415.
35. Wassarman,D.A. and Steitz,J.A. (1991) Structural analyses of the 7SK ribonucleoprotein (RNP), the most abundant human small RNP of unknown function. *Mol. Cell. Biol.*, **11**, 3432–3445.
36. van Zon,A., Mossink,M.H., Schoester,M., Scheffer,G.L., Scheper,R.J., Sonneveld,P. and Wiemer,E.A. (2002) Structural domains of vault proteins: a role for the coiled coil domain in vault assembly. *Biochem. Biophys. Res. Commun.*, **291**, 535–541.
37. Deutscher,S.L., Harley,J.B. and Keene,J.D. (1988) Molecular analysis of the 60-kDa human Ro ribonucleoprotein. *Proc. Natl Acad. Sci. USA*, **85**, 9479–9483.
38. Varani,G. and Nagai,K. (1998) RNA recognition by RNP proteins during RNA processing. *Annu. Rev. Biophys. Biomol. Struct.*, **27**, 407–445.
39. Whittaker,C.A. and Hynes,R.O. (2002) Distribution and evolution of von Willebrand/integrin A domains: widely dispersed domains with roles in cell adhesion and elsewhere. *Mol. Biol. Cell*, **13**, 3369–3387.
40. Pruijn,G.J., Slobbe,R.L. and van Venrooij,W.J. (1991) Analysis of protein–RNA interactions within Ro ribonucleoprotein complexes. *Nucleic Acids Res.*, **19**, 5173–5180.